

WJ Landis
R Jacquet
J Hillyer
E Lowder
A Yanke
L Siperko
S Asamura
H Kusuhara
M Enjo
S Chubinskaya
K Potter
N Isogai

Design and assessment of a tissue-engineered model of human phalanges and a small joint

Authors' affiliations:

William J. Landis, Robin Jacquet, Jennifer Hillyer, Elizabeth Lowder, Adam Yanke, Lorraine Siperko, Department of Biochemistry and Molecular Pathology, Northeastern Ohio Universities College of Medicine, Rootstown, OH, USA
Shinichi Asamura, Hirohisa Kusuhara, Mitsuhiro Enjo, Noritaka Isogai, Kinki University School of Medicine, Osaka, Japan
Susan Chubinskaya, Rush Medical Center, Chicago, IL, USA
Kimberlee Potter, Armed Forces Institute of Pathology, Washington, DC, USA

Correspondence to:

William J. Landis
Department of Biochemistry and Molecular Pathology
Northeastern Ohio Universities College of Medicine
4209 State Route 44
Rootstown
OH 44272-0095 USA
Tel.: +1 330 325 6685
Fax: +1 330 325 5915
E-mail: wjl@neoucom.edu

Dates:

Accepted 10 August 2005

To cite this article:

Orthod Craniofacial Res **8**, 2005; 303–312
Landis WJ, Jacquet R, Hillyer J, Lowder E, Yanke A, Siperko L, Asamura S, Kusuhara H, Enjo M, Chubinskaya S, Potter K, Isogai N:
Design and assessment of a tissue-engineered model of human phalanges and a small joint
Copyright © Blackwell Munksgaard 2005

Structured Abstract

Authors – Landis WJ, Jacquet R, Hillyer J, Lowder E, Yanke A, Siperko L, Asamura S, Kusuhara H, Enjo M, Chubinskaya S, Potter K, Isogai N.

Objectives – To develop models of human phalanges and small joints by suturing different cell-polymer constructs that are then implanted in athymic (nude) mice.

Design – Models consisted of bovine periosteum, cartilage, and/or tendon cells seeded onto biodegradable polymer scaffolds of either polyglycolic acid (PGA) or copolymers of PGA and poly-L-lactic acid (PLLA) or poly- ϵ -caprolactone (PCL) and PLLA. Constructs were fabricated to produce a distal phalanx, middle phalanx, or distal interphalangeal joint.

Setting and Sample Population – Studies of more than 250 harvested implants were conducted at the Northeastern Ohio Universities College of Medicine.

Experimental Variable – Polymer scaffold, cell type, and implantation time were examined.

Outcome Measure – Tissue-engineered specimens were characterized by histology, transmission electron microscopy, *in situ* hybridization, laser capture microdissection and qualitative and quantitative polymerase chain reaction analysis, magnetic resonance microscopy, and X-ray microtomography.

Results – Over periods to 60 weeks of implantation, constructs developed through vascularity from host mice; formed new cartilage, bone, and/or tendon; expressed characteristic genes of bovine origin, including type I, II and X collagen, osteopontin, aggrecan, biglycan, and bone sialoprotein; secreted corresponding proteins; responded to applied mechanical stimuli; and maintained shapes of human phalanges with small joints.

Conclusion – Results give insight into construct processes of tissue regeneration and development and suggest more

complete tissue-engineered cartilage, bone, and tendon models. These should have significant future scientific and clinical applications in medicine, including their use in plastic surgery, orthopaedics, craniofacial reconstruction, and teratology.

Key words: bone; cartilage; joints; phalanges; tendon; tissue-engineering

Introduction

The science of tissue engineering combines basic principles from biology, chemistry, physics and engineering to construct living tissues from their cellular components. A fundamental objective of this relatively new field of study is the medical application of fabricated tissues for the augmentation or replacement of congenitally defective, impaired, injured or otherwise damaged human tissue (1–3). At the present time, tissue engineering has advanced the design and development of many biological tissues, including aorta, bladder, skin, breast, muscle, bone, cartilage and tendon (4–12), and this area of scientific endeavor appears to have the potential for even wider applications in many medical specialties.

Engineered tissues have been investigated to determine their biocompatibility and biological, chemical and physical correlation with their counterpart naturally occurring tissues, their biostability, integration into host material and eventual restoration of normal structure and function (1–11). In this regard, this laboratory is developing models of human phalanges and small joints by suturing different cell–polymer constructs that are then implanted and elaborated in athymic mice. The models presently consist of bovine periosteum, cartilage and/or tendon cells seeded onto biodegradable polymer scaffolds. The latter may be comprised of either polyglycolic acid (PGA) or polymer blends of PGA and poly-L-lactic acid (PLLA) or poly- ϵ -caprolactone (PCL) and PLLA and they serve to support and enhance osteoblast, chondrocyte and tenocyte growth and subsequent development. These constructs are designed as a distal phalanx, middle phalanx or distal interphalangeal joint.

Careful and thorough characterization of the structure, chemistry and biology of the constructs is a clear requirement for understanding the means for their formation and the fundamental basis for their biocompatibility and other properties. A number of

diverse methodologies have thereby been applied in this context to investigate the variety of physical, chemical and biological properties of these models of tissue-engineered human phalanges and a small joint. This paper summarizes the previous and current studies describing the models and the results obtained by assessing them. The outcome of the investigation shows vascularization from the host mice as underlying the development of the constructs; formation of cartilage, bone and tendon in the models; gene expression of bovine type I, II and X collagens, osteopontin, aggrecan, biglycan and bone sialoprotein by the cells comprising the models; synthesis and secretion of the proteins corresponding to the characteristic genes; response to applied mechanical force and maintenance of the initial construct shapes throughout the period of their implantation in the mice. These data provide an understanding of some of the means for construct growth and development and additionally point toward further studies that hopefully will lead to direct clinical applications for these tissue-engineered models.

Materials and methods

Many of the basic techniques and approaches for fabricating and assessing the tissue-engineered phalangeal-joint constructs of interest have been published. They will be described here briefly as necessary with appropriate literature citations. The analytical methods include histology, transmission electron microscopy, *in situ* hybridization, laser capture microdissection (LCM) and qualitative and quantitative polymerase chain reaction (PCR) analysis, magnetic resonance microscopy (MRM) and X-ray microtomography (XMT).

Construct formation

Scaffold materials for the seeding of relevant cell types of interest were synthetic and biodegradable PGA, PLLA

and PCL (2,3,9–11). PGA was obtained from Albany International (Mansfield, OH, USA) or the Gunze Company (Kyoto, Japan) as non-woven mesh composed of 15 μm diameter fibers with inter-fiber pore spacing of $\sim 75\text{--}100 \mu\text{m}$. It supported inoculation and growth of either bovine chondrocytes or tenocytes (10,11). PLLA (Polysciences, Warrington, PA, USA) having fiber diameter and pore sizes comparable to PGA was blended with the latter and used for a scaffold with bovine periosteal cells.

In some experiments, PCL fibers (Gunze Co., Kyoto, Japan) (3,12) were copolymerized with PLLA for supporting periosteum.

Tissues from the shoulders of normal 4- to 6-week-old calves were obtained immediately on slaughter (Mahan Packing Co., Warren, OH, USA) and consisted of fresh periosteum, articular cartilage and tendon (10). Narrow strips of the periosteum were wrapped about the PGA/PLLA or PCL/PLLA scaffolds, which were molded in the shape of distal or middle phalanges of the human hand (10). The cambium layer of the tissue faced the copolymer and the strip was sutured as a ring of material completely encircling the scaffold. Articular cartilage was digested with 3% collagenase (type II; Worthington Biochemical, Freehold, NJ, USA) for 12 h to yield a heterogeneous mixture of bovine chondrocytes (10). Cells were cultured in Ham's F12 medium (Mediatech, Inc., Herndon, VA, USA) supplemented with 10% fetal bovine serum (FBS; Mediatech, Inc.). Cells were counted and diluted to 1.5×10^7 cells/ml and they were then seeded onto PGA sheets cut to a size of $10 \times 10 \times 2$ mm. Bovine tenocytes were isolated following the chondrocyte digestion procedure and these cells were similarly suspended and seeded onto PGA sheets (10). Each periosteum–copolymer construct was cultured for 1 week in M199 medium (Mediatech, Inc.) and each chondrocyte–PGA and tenocyte–PGA construct was cultured for 1 week in Ham's F12 medium. Supplements to all media included 10% FBS, an antibiotic–antimycotic and ascorbate, and the cultures were incubated at 37°C in 5% CO_2 (3,10,11).

After culture for a week, constructs were next created as relatively simple to more complicated engineered models for a human distal phalanx, a middle phalanx or a distal interphalangeal joint (10,11). The basic distal phalanx was formed by a single chondrocyte–PGA sheet sutured to one end of a periosteum–copolymer scaffold molded in a human distal phalanx shape.

Middle phalanx models were developed by suturing two chondrocyte–PGA sheets to a periosteum–copolymer scaffold, one sheet at each of its ends (the distal phalanx construct with a second chondrocyte–PGA sheet). In instances, a tenocyte–PGA sheet was sutured additionally to one of the chondrocyte–periosteum interfaces. The distal interphalangeal joint, the most complex of the models, was designed with a distal phalanx opposing a middle phalanx construct so that the respective articular surfaces (the chondrocyte–PGA sheets) of each model faced one another. An inert, thin silicone sheet was inserted between them, and a tenocyte–PGA sheet was wrapped and sutured about this portion of the full construct to approximate a joint between two bones of a human finger. The three types of composites were subsequently implanted under the dorsum of 4- to 6-week-old athymic (nude) mice and remained there for up to 60 weeks.

Histology

As noted earlier, histological analysis was utilized among a number of techniques for construct assessment. In this case, specimens retrieved after implantation were immersed in 10% neutral buffered formalin and embedded in paraffin. Sections 5–7 μm thick were treated variously with toluidine blue, hematoxylin and eosin, Safranin-O (13), Alizarin red, von Kossa, Gomori or other stains. These were used to identify matrix components (toluidine blue or hematoxylin and eosin) and the presence of proteoglycans secreted by cells (Safranin-O), calcium (Alizarin red), phosphate (von Kossa) or collagen (Gomori). Sections were examined and photographed by light microscopy.

Electron microscopy

Specimens were fixed in 4% paraformaldehyde, dehydrated in ethanol and embedded in Spurr resin (14,15). Sections 80–100 nm thick were prepared and stained with uranyl acetate and lead citrate to enhance ultrastructure of the engineered tissues examined by transmission microscopy (60–100 kV accelerating voltage).

In situ hybridization

Specimens were fixed in 4% paraformaldehyde and embedded in paraffin under stringent RNase-free

conditions (16–18). Antisense S³⁵-labeled oligonucleotide probes specific for bovine aggrecan, type II and X collagens, osteopontin, biglycan and bone sialoprotein were utilized for the studies (16). In addition, a similarly labeled probe for mouse decorin was investigated. The mouse decorin probe had no known bovine sequence and thereby provided critical discrimination between bovine and murine species (16). Specificity of all probes was compared with the sequence data from the DNA database, PC/GENE. The probes were hybridized to bovine tissue, mouse tissue and middle phalanx models of human phalanges implanted for 20 weeks in nude mice. After hybridization, sections were processed through autoradiography, counterstained with cresyl violet and examined and photographed by bright and dark field light microscopy. Epiphyseal and articular cartilage from metacarpals of normal newborn calves served as positive controls and the same tissue from the tibiae of normal 5-day-old mice was a negative control for hybridization studies with bovine probes. The identical cartilage specimens were negative and positive controls, respectively, for hybridization with the mouse decorin probe (16). A further negative control was the bovine type X collagen probe hybridized to bovine adult articular cartilage.

LCM and qualitative and quantitative PCR analysis

The procedure followed was that described in Landis et al. (19) and Jacquet et al. (20). Tissue-engineered constructs retrieved after implantation for up to 60 weeks were immediately placed in RNAlaterTM (Ambion, Austin, TX, USA) to preserve message and stored at -20°C . For processing, specimens were mounted on stubs with OCT and sections (5–7 μm thick) were obtained in a cryostat (-20°C) with the aid of a CryoJane device (Instrumedics, Inc., Hackensack, NJ, USA) to flatten them to slides (19,20). Sections on the slides were fixed in 70% ethanol and stained with eosin. Solutions used DEPC-treated water, and RNase Away (Molecular BioProducts, Inc., San Diego, CA, USA) maintained RNase-free conditions. LCM of individual cells or clusters of cells was performed with a Pixcell II LCM system (Arcturus Engineering, Mountain View, CA, USA). The technique utilized a low-energy laser pulse of 70 mW power and 2.5 ms duration to attach cells to a thin polymer transfer film on Cap-SureTM caps (Arcturus

Engineering) (19,20). The caps were then inserted into Eppendorf tubes containing lysis buffer and RNA was extracted from cells. RNA was next DNase-treated, reverse-transcribed to cDNA and then amplified by PCR using AmpliTaq[®] DNA polymerase (Applied Biosystems, Foster City, CA, USA) and primers specific for genes of interest (bovine type I and II collagens, osteopontin, osteocalcin, bone sialoprotein and aggrecan). For qualitative PCR (19), products were detected on ethidium bromide agarose gels. Both positive and negative controls were compared with experimental data. For quantitative real time PCR (20), analysis was performed using an ABI Prism 7700 Sequence Detector (Applied Biosystems, Foster City, CA, USA). GAPDH was utilized as a house-keeping gene for standardization. Final sample volumes for each control or experimental cDNA were 30 μl and contained SYBR[®] Green Master Mix (Applied Biosystems, Foster City, CA, USA), sterile water and 0.3 μM of each primer. Fluorescence measurements were used to generate a dissociation curve utilizing the software program v1.Ob1 (Applied Biosystems). From such melting curves, the degree of product purity was assessed by confirming the presence of a single peak at the known product melting temperature and the absence of any primer dimers. Amplicons were also electrophoresed on agarose gels to verify a single band at the appropriate molecular weight. The comparative C_T or standard curve method for relative quantitation of gene expression levels was used as outlined in User Bulletin 2 from Applied Biosystems. For the comparative C_T method, plots of ΔC_T versus log input concentration (~ 0.1 –20 ng control cDNA) were generated to demonstrate approximately equal efficiencies of target and reference (GAPDH) genes (20).

MRM

Whole middle phalanx constructs, retrieved from nude mice after implantation for 10 and 38 weeks, were placed in phosphate-buffered saline in sealed tubes. Non-invasive MRM measurements were performed at 37°C on a Bruker DMX spectrometer (Bruker Biospin MRI, Inc., Billerica, MA, USA) coupled to a wide-bore 9.4 T magnet. The field of view was $20 \times 10 \text{ mm}^2$, slice thickness was 1 mm and in-plane resolution was 78 μm . Measurements were

made of water proton longitudinal (T1) and transverse (T2) relaxation times, magnetization transfer rate (MTR) constant (k_m), proton density (PD) and lipid presence. All images were obtained with fat suppression. Further details of the procedures are given in Potter et al. (21,22).

XMT

Complete methodology has been described previously in Potter et al. (22). In summary, this non-invasive technique involved examination of intact, whole middle phalanx constructs, implanted for 10 and 38 weeks in nude mice. The specimens were wrapped in damp gauze and mounted in an X-TEK HMX microtomography system (X-TEK Systems, Ltd., Tring, UK) using tungsten as an X-ray source. The unit was operated at 90 kV and 255 mA with a 5 μm spot size. Imaging was through a CsI scintillator optically coupled to a cooled CCD camera, acquiring images of 1296 slices, 601 projections per slice and 1200 points per projection. The images were reconstructed in three dimensions and image pixel values were converted to quantitative concentrations of apatite, the characteristic mineral phase deposited in the constructs, by formulation using 3.18 g/cm^3 as the mineral density. Images were analyzed with user-defined procedures in Interactive Data Language (Research Systems, Inc., Boulder, CO, USA).

Constructs subjected to a mechanical force

Tissue-engineered middle phalanx models were tethered at their opposing ends with narrow strips of inert silicone that were then sutured to the neck (trapezius muscle) and tail (bony protuberance) of nude mice. Other middle phalanx models with silicone attachment as their counterparts were implanted without suturing to neck and tail tissues. In this manner, tethered constructs were designed to be directly affected by mechanical forces generated by ambulation of the mice in their cages and untethered constructs were presumed to be unaffected. Animals were sacrificed after 20 weeks of implantation and the constructs examined following fixation in 10% neutral buffered formalin and paraffin embedding. Sections of 5–7 μm thick were stained with toluidine blue, Safranin-O, Alizarin red, von Kossa or additional stains and photographed by light microscopy as described previously.

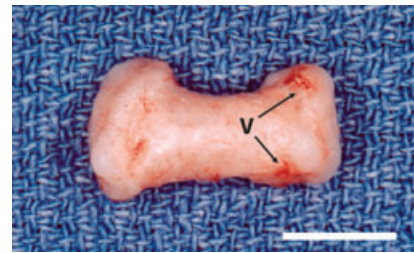


Fig. 1. An example of an intact tissue-engineered middle phalanx model implanted for 20 weeks in a nude mouse. The construct consists of two chondrocyte-seeded PGA sheets sutured at each end of a central periosteum-wrapped PCL/PLLA copolymer. This macroscopic view shows vascular networks (V) over the surface of the construct. Bar, 1 cm.

Results

Fig. 1 illustrates a typical tissue-engineered model of a human phalanx, in this instance a middle phalanx consisting of a scaffold of PCL/PLLA wrapped with bovine periosteum and sutured at each of its ends with a bovine chondrocyte-seeded PGA sheet. The whole mount (Fig. 1) shows that the construct, after 40 weeks of implantation, retains its original shape and dimensions of a human middle phalanx and has a red tinge over parts of its surface. On dissection (Fig. 2), the model appears to consist of smooth, glistening material at its ends and a complete structure in its midshaft region, which is red in color in particular areas. There is integration of tissue at the interface of the periosteum–PCL/PLLA and chondrocyte-seeded PGA sheets.

Histological staining (Figs 3–6) demonstrates that such constructs are comprised of bone and cartilage after at least 40 weeks of implantation in athymic mice. The end regions of the models are comprised exclusively of chondrocytes and they secrete a matrix rich in proteoglycans as indicated by Safranin-O staining

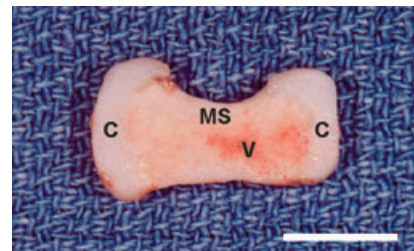


Fig. 2. The bisected model of Fig. 1 reveals smooth cartilage (C) at the extremes of the midshaft (MS). There is notable vascularization (V) within the shaft, as detected by a red coloring to the construct. An interface can be distinguished between cartilage and the shaft, but it is not prominent and as such suggests good integration between the tissues comprising these portions of the model. Bar, 1 cm.

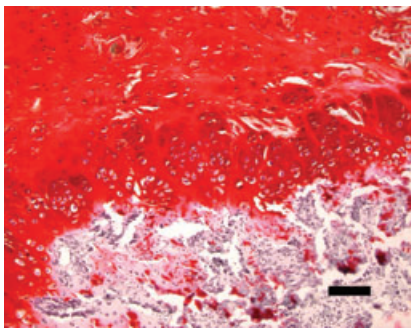


Fig. 3. A representative chondrocyte-seeded PGA scaffold region from a 40-week middle phalanx construct shows numerous cells and a secreted matrix prominently stained by Safranin-O to reveal proteoglycans. The cells have now organized into columns resembling a normal epiphyseal growth plate developing in vertebrate digits and long bones. Bar, 100 μm .

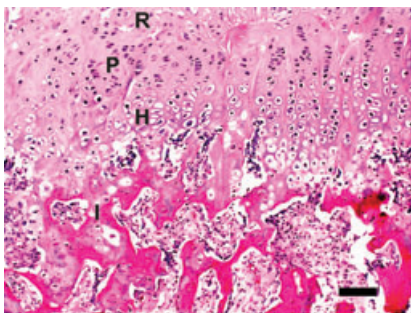


Fig. 4. The midshaft regions of a middle phalanx implanted for 38 weeks contain chondrocytes that undergo replacement to osteoblasts and bone through a putative endochondral process. This example is taken at the interface (I) between a chondrocyte-seeded PGA scaffold and a periosteal-wrapped PCL/PLLA copolymer. Note the indistinguishable junction and smooth integration of cells and matrix between the two previously sutured segments of the construct. Resting (R), proliferating (P), and hypertrophic (H) chondrocytes are clearly observed and those in hypertrophic zones are arranged in cell columns. The section has been stained with hematoxylin and eosin. Bar, 100 μm .

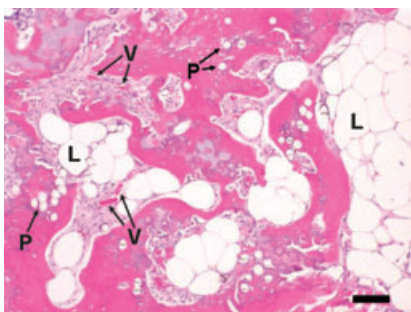


Fig. 5. Histology of a middle phalanx construct after 38 weeks of implantation reveals lipid deposits (L) and several vascular channels (V) in the midshaft region of the model. Some remnants of the scaffold polymer (P) are found in the specimen. The section has been stained with hematoxylin and eosin. Bar, 100 μm .

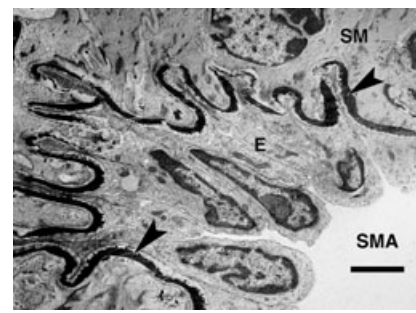


Fig. 6. Electron microscopy of a middle phalanx model following implantation for 20 weeks shows vasculature characterized by a small muscular artery (SMA) developed within the construct midshaft. The elastic laminae (arrowheads), endothelial cells (E) and smooth muscle (SM) of the artery are present in this section stained with uranyl acetate and lead citrate. Bar, 2 μm .

(Fig. 3). There is an intact chondro-osseous junction at the interfaces of what had been a separate periosteum–PCL/PLLA scaffold sutured to chondrocyte-seeded PGA sheets at the time of implantation (Figs 2 and 4). Osteoblasts and chondrocytes comprise the central shaft of the constructs, originally the site around which periosteum had been wrapped and sutured. A transition from cartilage to bone is inferred to occur in the construct midshaft, evidenced by morphology suggestive of an endochondral sequence in which the chondrocytes become hypertrophic, are resorbed and are replaced by osteoblasts (Fig. 4). With increasing time of implantation, the chondrocytes appearing within the ends of the constructs form a rudimentary growth plate in these regions, characterized by an arrangement and organization of the cells in generally parallel columns (Figs 3 and 4). Deeper regions of this plate contain progressively larger cells and lacunae compared to counterparts located in superficial portions of the plate (Fig. 4). Vascular channels and lipid deposits punctuate the midshaft of the middle phalanx models (Fig. 5).

Transmission electron microscopy confirms the presence of osteoblasts and chondrocytes in various areas of the constructs (data not shown) and also demonstrates cells and ultrastructure comprising a vasculature that pervades the models. In this regard, many capillaries, small muscular arteries and other vessels appear throughout the midshaft portion of the model phalanges and these hold erythrocytes, macrophages and other cells [Fig. 6; see (15)]. The vasculature itself is found consisting in part of type I collagen, endothelium, elastic laminae and additional structural elements (Fig. 6).

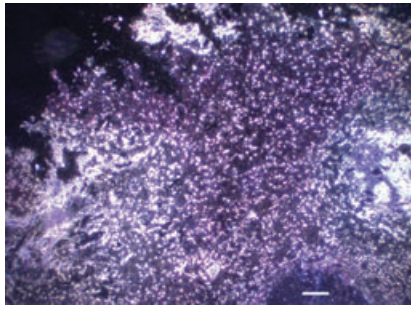


Fig. 7. *In situ* hybridization of a middle phalanx model implanted for 20 weeks in a nude mouse. This image taken with dark field photomicroscopy shows the positive reaction of a bovine-specific aggrecan probe hybridized to the cartilaginous portion of the construct. The section was stained with cresyl violet. This example is one of a complete series of *in situ* hybridization reactions utilizing bovine- and murine-specific probes with appropriate controls applied to similar tissue-engineered constructs and normal bovine and murine tissues (16). Only bovine-specific probes (for type II and X collagens, osteopontin, biglycan and bone sialoprotein, in addition to aggrecan) yield positive message and tissue-specific localization on hybridization to the constructs. Bar, 25 μ m.

Results of *in situ* hybridization demonstrate that all the oligonucleotide probes investigated are both tissue- and species-specific with respect to their positive and negative controls [data not shown; see (16)]. When hybridized to middle phalanx constructs, each bovine-specific probe gives positive message and tissue-specific localization within the cartilaginous and midshaft portions of the tissue-engineered models. Expression of bovine-specific type X collagen is found in epiphyseal cartilage in regions destined to become hypertrophic and calcified tissue. The mouse-specific decorin probe

yields no message on hybridization to the constructs. A representative microscopic image of these *in situ* hybridization studies is presented in Fig. 7.

In situ hybridization results are being supported by data currently obtained from LCM and PCR analysis. These studies to date show that, compared to appropriate controls, primers specific for bovine type II collagen and aggrecan among the other genes of interest noted previously may be identified, localized and quantitated from individual or small clusters of chondrocytes comprising cartilage covering the ends of middle phalanx models implanted for 20 weeks in nude mice (Table 1).

The two complementary, non-invasive techniques of MRM and XMT reveal spatial and temporal development of various tissue elements within tissue-engineered middle phalanx models following implantation for 10 and 38 weeks in athymic mice. Fig. 8 illustrates, for example, the quantitative T1 and PD images obtained from 3D MRM datasets and a corresponding XMT image of a 38-week specimen. The correlative presence of organic and inorganic components detected by MRM and XMT, respectively, is clearly observed. In addition, vascular channels traversing the model are delineated by each of the techniques (Fig. 8), and bound and free water and the presence of lipid deposits may be ascertained [data not shown; see (22)].

Figs. 9 and 10 compare representative cartilage regions over the ends of two middle phalanx models retrieved from nude mice after 20 weeks of implantation.

Table 1. Detection and relative expression of bovine aggrecan and type II collagen in a tissue-engineered middle phalanx model implanted for 20 weeks in a nude mouse

Cell type*	Aggrecan total control bone RNA (ng)	Melting curve analysis 81°C	GAPDH total control bone RNA (ng)	Melting curve analysis 82°C	Aggrecan normalized to GAPDH
Chondrocytes	0.08	80.0	0.00152	81.1	52.63
Osteoblasts	0.01	79.8	0.00024	81.3	41.67
Cell type	Aggrecan relative to chondrocytes	Type II collagen total control bone RNA (ng)	Melting curve analysis 79°C		
Chondrocytes	1.00	0.002	79.4		
Osteoblasts	0.79 [†]	0 [†]	0		

*300–500 chondrocytes or osteoblasts were isolated by laser capture microdissection and subjected to the standard curve analysis for relative quantitation of aggrecan and type II collagen gene expression levels. GAPDH was used as a reference gene. The approach is detailed in User Bulletin 2 from Applied Biosystems (Foster City, CA, USA).

[†]Data demonstrate expression of aggrecan and type II collagen in captured chondrocytes. No type II collagen expression is detected in osteoblasts. Measured relative aggrecan expression (0.79) in osteoblasts is sensitive to small changes in the small total aggrecan RNA (0.01 ng) and, as a result, likely may be an overestimation. On the other hand, laser-captured cells identified as osteoblasts may be immature precursor cells that could express aggrecan.

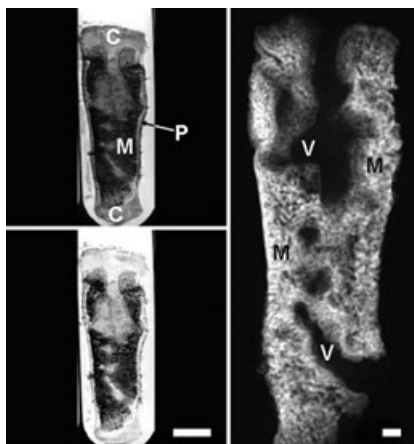


Fig. 8. Non-invasive magnetic resonance microscopy (MRM) and X-ray microtomography (XMT) of the same middle phalanx construct implanted for 38 weeks in a nude mouse. Quantitative T1 and PD images (upper and lower left panels, respectively) from MRM of a 1 mm thick sagittal slice show cartilage (C) at the construct ends, periosteal tissue (P) surrounding the construct midshaft and vascular channels invading the specimen. The degree of hydration of the sample, assessed by the level of image intensity, varies over the slice. The presence of water is marked by regions of high or bright intensity and hydration; the presence of mineral is detected by regions of low or dark intensity and hydration. The corresponding XMT image (right panel) shows the mineral (M) (high or bright intensity) comprising the construct. Unmineralized specimen regions, including vascular channels (V) and cartilage at the construct ends, have no intensity in XMT images. Bar, 5 mm (MRM images) and 1 mm (XMT image).

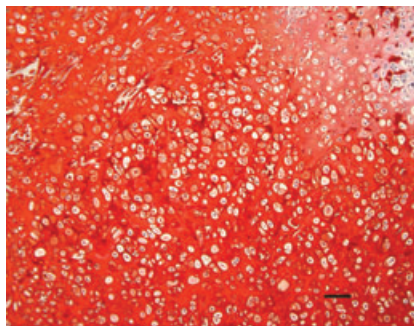


Fig. 9. A middle phalanx model retrieved after 20 weeks of implantation and tethered directly to muscle and bone of a host nude mouse typically contains abundant numbers of chondrocytes and rudimentary cell columns and demonstrates rich Safranin-O staining for proteoglycans. Bar, 100 μ m.

One of the animals harbored a construct having its proximal and distal ends tethered with silicone strips and sutured to the neck and hind regions, respectively, of the mouse (Fig. 9). The other animal incubated an untethered construct (Fig. 10). Compared to the latter, the tethered model has a generally higher content of proteoglycans as determined by Safranin-O staining and notable rudimentary organization of its constituent chondrocytes into cell columns. The tethered model also develops greater volumes of cartilage and posses-

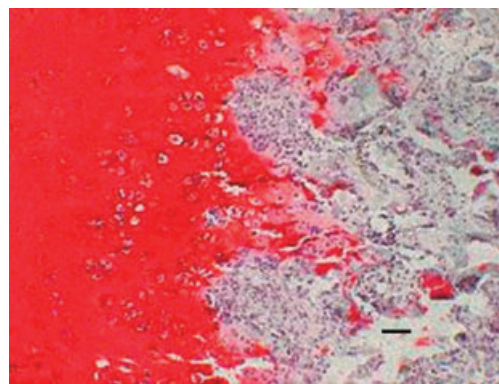


Fig. 10. A middle phalanx construct following implantation for 20 weeks without tethering contains fewer chondrocytes and cell columns compared to tethered counterparts. Proteoglycan content reflected by the intensity of Safranin-O staining is generally somewhat less than that observed in tethered specimens. Bar, 100 μ m.

ses more bone in its midshaft regions [data not shown; see reference (23)].

Discussion

This paper provides an overview of earlier and ongoing laboratory investigations concerned with the tissue engineering design and assessment of a model for human phalanges and a small joint. Ultimately, the development of the model is intended for functional human clinical application in combination with tissue-engineered muscle, nerve, blood vessels and skin that will be fabricated and integrated with the phalanges. Like current efforts to improve and expand the engineering of other tissues (4–9,24,25), such phalangeal constructs hopefully will be biocompatible and lead to complete restoration of structure and function of pathological, impaired or damaged human bone and small joints.

Tissue engineering of bone, cartilage and tendon has been studied previously (3,5,7,9,24,26–32, for example), but employing all three cell types in a single construct had not been reported until a few years ago (10). Results from that work have been extended as described above and summaries of the compiled data are noted subsequently. The relatively brief details presented in Materials and methods and in some of the Results section here may be found in greatly expanded form in several journal articles and book chapters already published and referenced here (3,10,11,15,16, 19–22).

To conclude, it is clear that the formation of tissue-engineered models of human phalanges and a small joint can be accomplished with selective placement of periosteum, chondrocytes and tenocytes onto appropriate biodegradable scaffolds. The shapes of the models can be maintained morphologically with combinations of PGA, PCL and PLLA, all of which support the bone, cartilage and tendon cells structurally and mechanically and help guide their three-dimensional development and organization into viable tissue. In this regard, the scaffolds also promote cell adhesion, migration, differentiation, proliferation and growth. The cells in turn establish, through gene expression and protein synthesis and secretion, extracellular matrices specific and characteristic to bone, cartilage and tendon. Additionally, the constructs form an apparent rudimentary cartilaginous growth plate in place of initial chondrocyte-seeded scaffolds at the ends of the models, contain bound and free water and lipid deposits and mineralize through the endochondral process of cartilage replacement with bone tissue.

Vascularization of the constructs is supplied by the host nude mice and leads to the presence of capillaries, small muscular arteries and other vessels in the periosteal and cancellous bone regions of phalanx models. Erythrocytes, endothelial and smooth muscle cells and elastic laminae of the muscular arteries, macrophages, collagen and additional cells and elements originating with the vasculature are detectable. These constituents within the models provide their oxygenation, nutrition, and mechanical integrity as well as the means for the degradation of their supporting polymer scaffolds by cellular intervention over time. While vascular components and nutrition originate from the mice in these tissue-engineering studies, the models maintain their initial bovine genotype throughout long implantation periods. *In situ* hybridization demonstrated positive reactions for several bovine-specific, but not murine-specific, probes that were individually incubated with the constructs. Finally, based on the studies in which middle phalanx models are tethered directly to the muscle and bone of host mice, it appears that chondrocyte structure, growth and organization are directed and enhanced by mechanical force. In this regard then, the constructs appear to respond to mechanical stimuli as do normally mineralizing tissues.

Taken together, these results show that the tissue-engineered models of phalanges and small joints

elaborate the form and morphology, maintain the ultrastructure and biochemical composition and adapt to mechanical force closely approximating those characteristics of their human counterparts. These data are extremely useful in understanding fundamental physical, chemical and biological processes governing the models. They are also important for gaining insight into the means for improving the constructs in terms of tissue regeneration and development and for applying the scientific findings as correlates for functional normal tissue. Work in these directions is continuing with an emphasis on clinical application for these tissue-engineered constructs in several fields.

Acknowledgements: This work was supported by National Institute of Health grants AR41452 (to WJL), AR39239 [a SCOR grant awarded to Dr K. Kuettner (Rush University Medical School) and supporting SC in part], and DE14453 (to KP) and a Hitech Research Center grant from the Ministry of Education, Culture, Sports, Science, and Technology, Japan (to NI). The authors are grateful for the bovine type II collagen and aggrecan sequences for *in situ* hybridization provided by Dr Linda Sandell (Washington University, St Louis, MO, USA), poly- ϵ -caprolactone for cell scaffolds from Dr Yoshito Ikada (Kyoto University, Kyoto, Japan), technical assistance with *in situ* hybridization from Ms Rita Mikhail (Rush Medical Center, Chicago, IL, USA), and computer graphics and media services from Ms Susan Benson and Ms Dolly Lock (Northeastern Ohio Universities College of Medicine, Rootstown, OH, USA). The authors thank Walter Horne, D.V.M., director, Comparative Medicine Unit, Northeastern Ohio Universities College of Medicine, and his staff members, Ms Lora Nicholson, Ms Susan Kissel, Ms Deborah Dutton, Ms Cindy Fobes, Mr Richard Rambacher, Mr John Ryznar, and Mr Mark Moser for their assistance, concern, and dedication with animal use and care.

References

1. Woolverton CJ, Fulton JA, Lopina ST, Landis WJ. Mimicking the natural tissue environment. In: Lewandrowski K-U, Wise DL, Trantolo DJ, Gresser JD, Yaszemski MJ, Altobelli DE, editors. *Tissue Engineering and Biodegradable Equivalents: Scientific and Clinical Applications*. New York, NY: Marcel Dekker; 2002. pp. 43–75.
2. Landis WJ, Jacquet R, Hillyer J, Zhang J, Siperko L, Chubinskaya S et al. The potential of tissue engineering in orthopaedics. *Orthop Clin North Am* 2005;**36**:97–104.
3. Isogai N, Asamura S, Higashi T, Ikada Y, Morita S, Hillyer J et al. Tissue engineering of an auricular cartilage model utilizing cultured chondrocyte-poly(L-lactide- ϵ -caprolactone) scaffolds. *Tissue Eng* 2004;**10**:673–87.
4. Pariente JL, Kim BS, Atala A. In vitro biocompatibility assessment of naturally derived and synthetic biomaterials using normal human urothelial cells. *J Biomed Mater Res* 2001;**55**:33–39.

5. Shum-Tim D, Stock U, Hrkach J, Shinoka T, Lien J, Moses M et al. Tissue engineering of autologous aorta using a new biodegradable polymer. *Ann Thorac Surg* 1999;**68**:2298–305.
6. Vaccariello MA, Javaherian A, Parenteau N, Garlick JA. Use of skin equivalent technology in a wound healing model. In: Morgan JR, Yarmush ML, editors. *Methods in Molecular Medicine: Tissue Engineering Methods and Protocols*. Vol. 18. Totowa, NJ: Humana Press; 1999. pp. 391–405.
7. Cao YL, Lach E, Kim TH, Rodriguez A, Arevalo CA, Vacanti CA. Tissue-engineered nipple reconstruction. *Plast Reconstr Surg* 1998;**102**:2293–8.
8. Vandenburg H, Shansky J, Del Totto M, Chromiak J. Organogenesis of skeletal muscle in tissue culture. In: Morgan JR, Yarmush ML, editors. *Methods in Molecular Medicine: Tissue Engineering Methods and Protocols*. Vol. 18. Totowa, NJ: Humana Press; 1999. pp. 217–25.
9. Tubo R, Binette F. Culture and identification of autologous human articular chondrocytes for implantation. In: Morgan JR, Yarmush ML, editors. *Methods in Molecular Medicine: Tissue Engineering Methods and Protocols*. Vol. 18. Totowa, NJ: Humana Press; 1999. pp. 205–15.
10. Isogai N, Landis WJ, Kim TH, Gerstenfeld LC, Upton J, Vacanti JP. Formation of phalanges and small joints by tissue engineering. *J Bone Joint Surg* 1999;**81-A**:306–16.
11. Isogai N, Landis WJ. Phalanges and small joints. In: Atala A, Lanza R, editors. *Methods of Tissue Engineering*. San Diego, CA: Academic Press; 2001. pp. 1041–7.
12. Hattori K, Tomita N, Tamai S, Ikada Y. Bioabsorbable thread for tight tying of bones. *J Orthop Sci* 2000;**5**:57–63.
13. Rosenberg L. Chemical basis for the histological use of Safranin-O in the study of articular cartilage. *J Bone Joint Surg* 1971;**53-A**:69–82.
14. Landis WJ. A study of calcification in the leg tendons from the domestic turkey. *J Ultrastruct Mol Struct Res* 1986;**94**:217–38.
15. Yanke A, Hillyer J, Killius J, Isogai N, Asamura S, Jacquet R et al. Vascularity of a tissue-engineered model of human phalanges. *Microsc Microanal* 2002;**8**:1024–5CD.
16. Chubinskaya S, Jacquet R, Isogai N, Asamura S, Landis WJ. Characterization of the cellular origin of a tissue-engineered human phalanx model by in situ hybridization. *Tissue Eng* 2004;**10**:1204–13.
17. Chubinskaya S, Huch K, Mikecz K, Cs-Szabo G, Hasty KA, Kuettner KE et al. Chondrocyte matrix metalloproteinase-8: up-regulation of neutrophil collagenase by interleukin-1 β in human cartilage from knee and ankle joints. *Lab Invest* 1996;**74**:232–40.
18. Chubinskaya S, Kuettner KE, Cole AA. Expression of matrix metalloproteinases in human normal and damaged articular cartilage from knee and ankle joints. *Lab Invest* 1999;**79**:1669–77.
19. Landis WJ, Jacquet R, Hillyer J, Zhang J. Analysis of osteopontin in mouse growth plate cartilage by application of laser capture microdissection and RT-PCR. *Connect Tissue Res* 2003;**44**:28–32.
20. Jacquet R, Hillyer J, Landis WJ. Analysis of connective tissues by laser capture microdissection and reverse transcriptase-polymerase chain reaction. *Anal Biochem* 2004;**337**:22–34.
21. Potter K, Leapman RD, Basser PJ, Landis WJ. Cartilage calcification studied by proton nuclear magnetic resonance microscopy. *J Bone Miner Res* 2002;**17**:652–60.
22. Potter K, Sweet DE, Anderson P, Isogai N, Asamura S, Kusuhara H, et al. Non-invasive studies of tissue-engineered phalanges by magnetic resonance microscopy and X-ray microtomography. *Bone* 2005 (in press).
23. Landis WJ, Jacquet R, Hillyer J, Asamura S, Isogai N. Effect of mechanical force on the development of a novel tissue-engineered model of human middle phalanges. *Proceedings of the Materials Research Society*. 2002.
24. Cao Y, Vacanti JP, Ma X, Paige KT, Upton J, Chowanski Z et al. Generation of neo-tendon using synthetic polymers seeded with tenocytes. *Transplant Proc* 1994;**26**:3390–2.
25. Hadlock T, Elisseeff J, Langer R, Vacanti J, Cheney M. A tissue-engineered conduit for peripheral nerve repair. *Arch Otolaryngol Head Neck Surg* 1998;**124**:1081–6.
26. Cima LG, Vacanti JP, Vacanti C, Ingber D, Mooney D, Langer R. Tissue engineering by cell transplantation using degradable polymer substrates. *J Biomech Eng* 1991;**113**:143–51.
27. Vacanti CA, Langer R, Schloo B, Vacanti JP. Synthetic polymers seeded with chondrocytes provide a template for new cartilage formation. *Plast Reconstr Surg* 1991;**88**:753–9.
28. Vacanti CA, Upton J. Tissue-engineered morphogenesis of cartilage and bone by means of cell transplantation using synthetic biodegradable polymer matrices. *Clin Plast Surg* 1994;**21**:445–62.
29. Kim WS, Vacanti JP, Cima L, Mooney D, Upton J, Puelacher WC et al. Cartilage engineered in predetermined shapes employing cell transplantation on synthetic biodegradable polymers. *Plast Reconstr Surg* 1994;**94**:233–7.
30. Sakata J, Vacanti CA, Schloo B, Healy GB, Langer R, Vacanti JP. Tracheal composite tissue engineered from chondrocytes, tracheal epithelial cells and synthetic degradable scaffolding. *Transplant Proc* 1994;**26**:3309–10.
31. Kim TH, Jannetta C, Vacanti JP, Upton J, Vacanti CA. Engineered bone from polyglycolic acid polymer scaffold and periosteum. *Mater Res Soc Symp Proc* 1995;**394**:91–97.
32. Obradovic B, Martin I, Padera RF, Treppo S, Freed LE, Vunjak-Novakovic G. Integration of engineered cartilage. *J Orthop Res* 2001;**19**:1089–97.

Copyright of Orthodontics & Craniofacial Research is the property of Blackwell Publishing Limited. The copyright in an individual article may be maintained by the author in certain cases. Content may not be copied or emailed to multiple sites or posted to a listserv without the copyright holder's express written permission. However, users may print, download, or email articles for individual use.